CURVED PIN OR TANG FK 2670.20 – TIN BRONZE – LATE BRONZE AGE – SWITZERLAND

Artefact name Curved pin or tang FK 2670.20

Authors Marianne. Senn (Empa, Dübendorf, Zurich, Switzerland) & Christian. Degrigny (HE-Arc CR, Neuchâtel, Neuchâtel, Switzerland)

Url /artefacts/1574/

The object

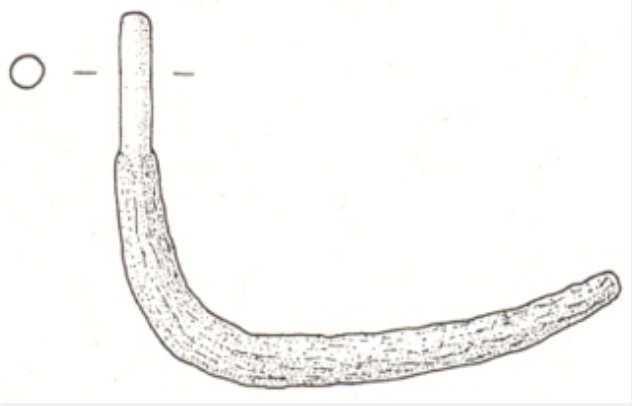

Fig. 1: Curved pin or tang (after Fischer 1997, plate 43),

Credit HE-Arc CR.

Description and visual observation

Description of the artefact Curved pin or tang (Fig. 1). The metal is covered with black corrosion products attributed to a burning process mixed with green corrosion products. Dimensions: L = 114mm; Ø = 4.6mm; WT = 16.7g.

Type of artefact Not defined

Origin Steinmöri, Neftenbach / Dorf Neftenbach, Zurich, Switzerland

Recovering date Excavation in 1991?, grave 18

Chronology category Late Bronze Age

chronology tpq 1400 B.C.

chronology taq 1300 B.C.

Chronology comment	14th century BC, Bronze Age D
Burial conditions / environment	Soil
Artefact location	Kantonsarchäologie, Dübendorf, Zurich
Owner	Kantonsarchäologie, Dübendorf, Zurich
Inv. number	FK 2670.20
Recorded conservation data	N/A

Complementary information

None.

Study area(s)

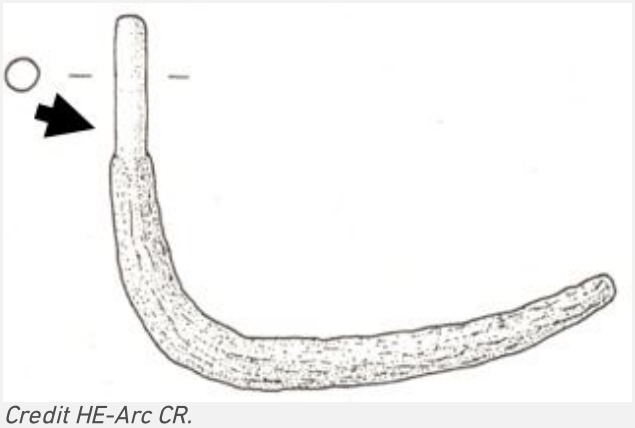

Credit HE-Arc CR.

Fig. 2: Location of sampling area,

Binocular observation and representation of the corrosion structure

None.

MiCorr stratigraphy(ies) – Bi

Sample(s)

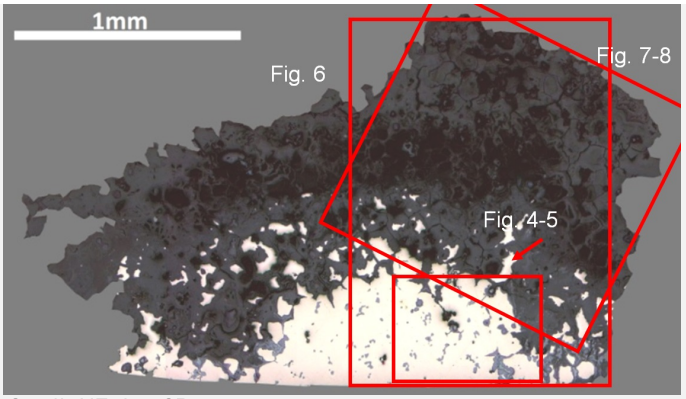

Credit HE-Arc CR.

Fig. 3: Micrograph of the cross-section of the sample taken from the curved pin or tang showing the location of Figs. 4 to 8,

Description of sample	Several samples were taken. Only one is presented here (Fig. 2). The sample (Fig. 3) is a section from the pin (or tang). The metal is covered by a thick corrosion crust (blue layer adhering to the metal, topped by a green layer mixed with black corrosion products - Museum report (1992)). Dimensions: L = 1.8mm; W = 1.2mm.
Alloy	Tin Bronze
Technology	Secondary recrystallization (produced by burning)
Lab number of sample	MAH 92-5-4-002
Sample location	Musées d'art et d'histoire, Genève, Geneva
Responsible institution	Musées d'art et d'histoire, Genève, Geneva
Date and aim of sampling	1992, examination of metallography examination

Complementary information

None.

Analyses and results

Analyses performed:
Metallography (etched with ferric chloride reagent), Vickers hardness testing, EPMA/WDS, SEM/EDS.

Non invasive analysis

None.

Metal

The remaining metal is a tin bronze (Table 1) with copper sulphide inclusions that contain some Fe (Figs. 4 and 5, Table 2). After etching, the tin bronze shows polygonal grains with few twins (Fig. 5). The grain size varies between 70 and 180µm indicating grain growth due to an extended or excessively hot annealing process. The copper sulphide inclusions appear in blue. The average hardness of the metal is HV1 70.

Elements	Cu	Sn	Pb	As	Sb	Fe	Zn	Ag	Au	Co	Bi	Ni	S
mass%	89.94	8.11	0.63	0.41	0.29	0.24	0.13	0.1	0.1	0.04	0.01	<	n. d.

Table 1: Chemical composition of the metal (<: below the detection limit). Method of analysis: EPMA/WDS, Lab Department of Materials, University of Oxford.

Elements	S	Fe	Cu	Total
Dark-blue inclusion	21	2.8	77	102

Table 2: Chemical composition (mass %) of the dark-blue inclusions on Fig. 4. Method of analysis: SEM/EDS, Laboratory of Analytical Chemistry, Empa.

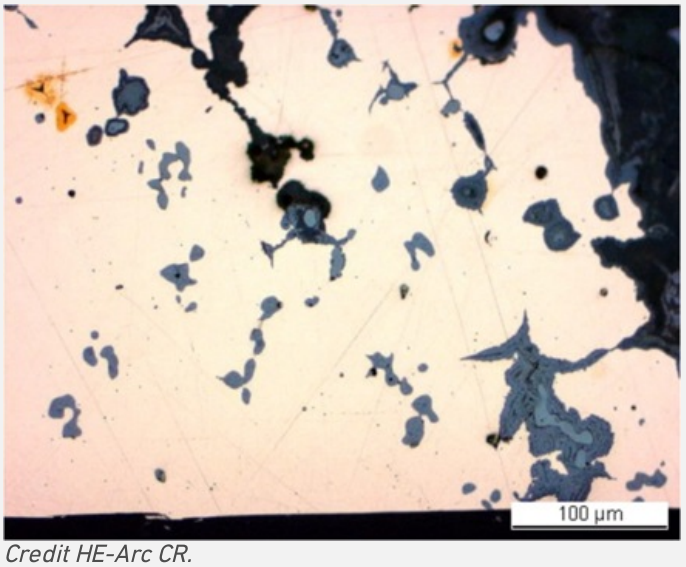

Credit HE-Arc CR.

Fig. 4: Micrograph of the metal sample from Fig. 3 (detail), unetched, bright field. In pink the metal, in light-blue the copper sulphide inclusions and in dark- blue corrosion products,

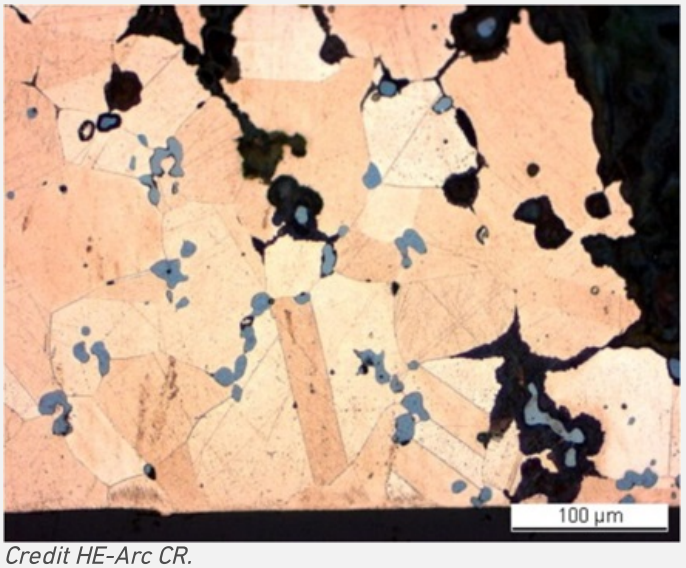

Credit HE-Arc CR.

Fig. 5: Micrograph of the metal sample from Fig. 3 (same as Fig. 4), etched, bright field. In pink the metal with few twins, in black the resin and the corrosion products, in light-blue the copper sulphide inclusions,

Microstructure	Large polygonal grains with few twins
First metal element	Cu
Other metal elements	Fe, Co, Zn, As, Ag, Sn, Sb, Pb

Complementary information

None.

Corrosion layers

The corrosion crust has an average thickness of 500µm but can in areas be much thicker (Fig. 3). It is divided in two layers. The inner layer is itself divided in two sub-layers: a thin light-grey sub-layer at the interface with the remaining metal surface (CP4, in bright field) which appears red-orange in polarised light (Fig. 6) topped by a medium-grey sub-layer (in bright field) that contains remnant metal (CP3). It turns dark-blue in polarised light (Fig. 6). The outer corrosion layer can also be divided into two sub-layers: a porous sub-layer (CP2) followed by a dark-grey sub-layer in which crystals are outlined by cracks (CP1, in bright field). Under polarized light, the latter turns blue-green while on top it appears olive and brown (Fig. 6). Chemically the corrosion crust is Sn enriched and Cu-depleted (Table 3, Figs. 7 and 8). The maximum of the Sn enrichment occurs on the outer olive and brown sub-layer (CP1). The corrosion layer also contains P, Si, C and O. Inclusions containing Fe or Ag can be found in the corrosion crust (Figs. 7 and 8).

Elements	O	Cu	Sn	Si	P	Fe	Pb	S	Cl	Total
CP1, outer corrosion layer	27	17	57	1	2	1	1	<	<	106
CP3, inner corrosion layer	39	27	26	1	3	<	<	<	<	96
Remnant metal in CP3	<	88	8	<	<	<	<	<	<	96

Table 3: Chemical composition (mass %, <: below the detection limit) of the corrosion crust from Fig. 6. Method of analysis: SEM/EDS, Laboratory of Analytical Chemistry, Empa.

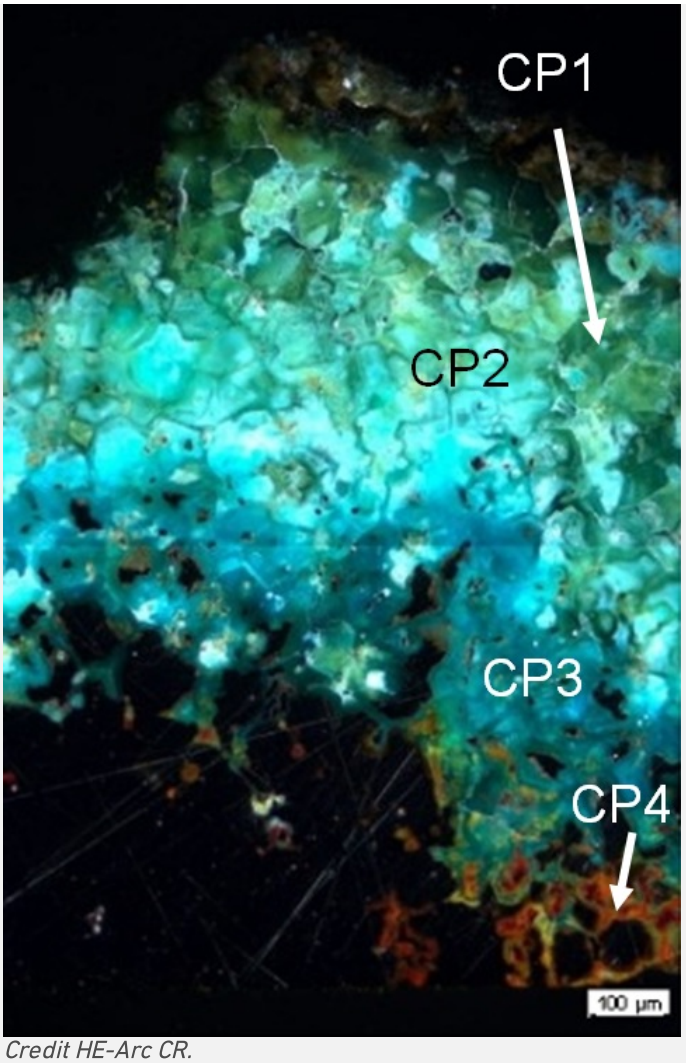

Fig. 6: Micrograph of the metal sample from Fig. 3 (detail) and corresponding to the MiCorr stratigraphy of Fig. 9, unetched, polarised light. At the metal - corrosion products interface the colour of the corrosion layer is dark-blue, changing to green-blue in the outer part. The top surface of the corrosion crust is olive to brown,

Credit HE-Arc CR.

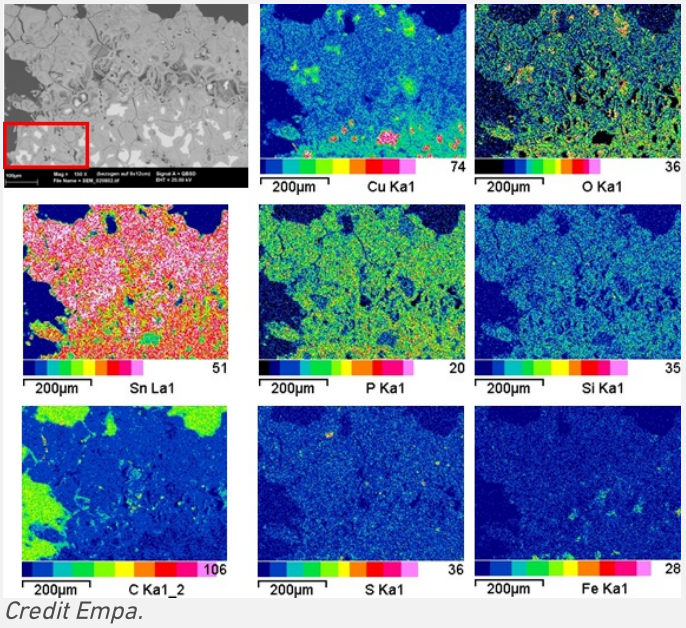

Fig. 7: SEM image, BSE-mode, and elemental chemical distribution of the selected area from Fig. 3 (due to repolishing before SEM/EDX investigation, the SEM image is slightly different from the area indicated in Fig. 3). The rectangle in the SEM image marks the detail mapping of Fig 8. Method of examination: SEM/EDS, Laboratory of Analytical Chemistry, Empa,

Credit Empa.

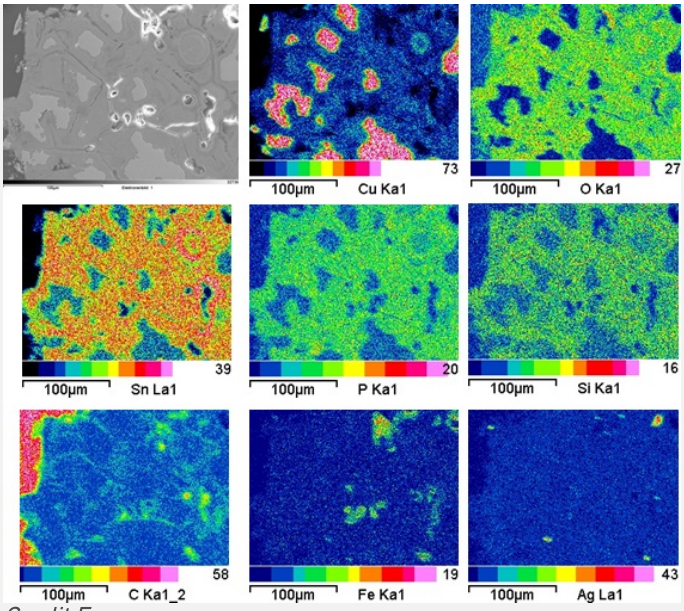

Credit Empa.

Fig. 8: SEM image, SE-mode, and elemental chemical distribution of the selected area from Fig. 7. Method of examination: SEM/EDS, Laboratory of Analytical Chemistry, Empa,

Corrosion form	Uniform - intergranular
Corrosion type	Type II (Robbiola)

Complementary information

None.

MiCorr stratigraphy(ies) – CS

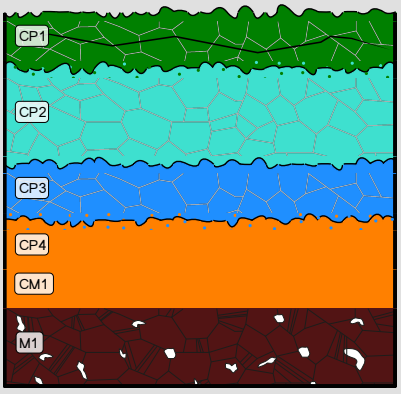

Fig. 9: Stratigraphic representation of the sample taken from the curved pin or tang in cross-section (dark field) using the MiCorr application. The characteristics of the strata are only accessible by clicking on the drawing that redirects you to the search tool by stratigraphy representation. This representation can be compared to Fig. 6, Credit HE-Arc CR.

Synthesis of the binocular / cross-section examination of the corrosion structure

None.

Conclusion

The tin bronze was exposed to an extended or excessively hot annealing process. This, combined with the extreme thickness of the corrosion crust and the dark surface, confirms that the object originates from a fire burial context. At the metal - corrosion crust interface some copper oxide (cuprite?) occurs. On top copper carbonates (azurite or malachite?) are mixed with tin oxide (cassiterite/SnO2?). Tin oxide dominates in the brown-black extremely Sn-rich outer layer. The P-enrichment in the whole corrosion layer may be due to an environment rich in organic material (for example bones). The original surface of the metal has been destroyed, presenting a type 2 corrosion layer after Robbiola et al. 1998.

References

References on object and sample

Reference object

1. Fischer, C. (1997) Innovation und Tradition in der Mittel- und Spätbronzezeit. Monographien der Kantonsarchäologie Zürich 28 (Zürich und Egg), 181 and plate 43.

Reference sample

2. Fischer, C. (1997) Innovation und Tradition in der Mittel- und Spätbronzezeit. Monographien der Kantonsarchäologie Zürich 28 (Zürich und Egg), 96.
3. Rapport d'examen 92-5-4 (Schweizer, F. and degli Agosti, M.), Laboratoire Musées d'art et d'histoire, Geneva GE (1992).

References on analytic methods and interpretation

4. Robbiola, L., Blengino, J-M., Fiaud, C. (1998) Morphology and mechanisms of formation of natural patinas on archaeological Cu-Sn alloys, Corrosion Science, 40, 12, 2083-2111.